Combined Infrared Stereo and Laser Ranging Cloud Measurements from Shuttle Mission STS-85

REDGIE S. LANCASTER

Goddard Earth Science and Technology Center, University of Maryland, Baltimore County, Baltimore, Maryland

JAMES D. SPINHIRNE

NASA Goddard Space Flight Center, Greenbelt, Maryland

KATHRINE F. MANIZADE

Science Systems and Applications, Inc., Lanham, Maryland

(Manuscript received 27 November 2001, in final form 30 April 2002)

ABSTRACT

Multiangle remote sensing provides a wealth of information for earth and climate monitoring, such as the ability to measure the height of cloud tops through stereoscopic imaging. Further, as technology advances so do the options for developing spacecraft instrumentation versatile enough to meet the demands associated with multiangle measurements. One such instrument is the infrared spectral imaging radiometer, which flew as part of mission STS-85 of the space shuttle *Columbia* in 1997 and was the first earth-observing radiometer to incorporate an uncooled microbolometer array detector as its image sensor. Specifically, a method for computing cloud-top height with a precision of ±620 m from the multispectral stereo measurements acquired during this flight has been developed, and the results are compared with coincident direct laser ranging measurements from the shuttle laser altimeter. Mission STS-85 was the first space flight to combine laser ranging and thermal IR camera systems for cloud remote sensing.

1. Introduction

Satellite meteorology contributes a wealth of information about the atmosphere primarily through the collection and dissemination of visible and infrared imagery. This imagery is acquired using radiometers included on geosynchronous and polar-orbiting spacecraft and provides operational data about global and regional weather patterns critical to a large portion of society. However, this field of research is built upon atmospheric remote sensing and the information acquired using these techniques is incomplete. An example of one such shortcoming in the imagery obtained from meteorological satellites is that the vertical dimension of the scene is only indirectly inferred. This may not be of great practical import in general, but it is difficult to deny the importance of the vertical dimension of the atmosphere for many aspects of predictive climate and meteorological research.

Different remote sensing methods can be combined to obtain a more complete picture of the atmosphere such as with infrared observations that couple radiometric imagery of a cloud at several wavelengths with an independent knowledge of the atmospheric temperature to arrive at a height estimate. Several methods of this sort have been developed that include the IR window technique, the CO_2/IR window ratio technique, and the H_2O/IR window intercept method (Nieman et al. 1993). The focus of the current work is also the retrieval of cloud-top height from infrared satellite imagery. However, the approach adopted herein departs from these methods and utilizes a purely geometric retrieval of height that recovers the vertical dimension of the imagery through the application of stereoscopic analysis.

Meteorologists have long recognized the value of using satellite imagery at visible wavelengths to obtain stereo height measurements of cloud tops. The earliest examples date back to the NASA Nimbus Technology satellite program (Ondrejka and Conover 1966; Kikuchi and Kasai 1968) of the early 1960s and the unmanned flight of Apollo 6 (Whitehead et al. 1969; Shenk et al. 1975) in 1968. With the launch of the National Aeronautics and Space Administration (NASA) environmental satellites *SMS-1* and *SMS-2* in 1974 and 1975,

Corresponding author address: Dr. Redgie Lancaster, NASA Goddard Space Flight Center, Code 912, Greenbelt, MD 20771.
E-mail: lancaster@virl.gsfc.nasa.gov

the focus of stereo remote sensing began to shift toward the use of imagery obtained from geosynchronous orbit (Bristor and Pichel 1974) using multiple spin-scan radiometers during specialized coordinated experiments (Minzner et al. 1978). This continued with the launch of the National Oceanic and Atmospheric Administration (NOAA) Geostationary Observational Environmental Satellite (GOES) *GOES-East* and *GOES-West* satellites in the latter 1970s (Hasler 1981) and included combinations such as the *GOES-West* and the Japanese *GMS-1* geosynchronous satellite (Fujita 1982), and the *GOES-East* and TIROS-N polar-orbiting satellites (Hasler et al. 1983).

These experiments formed the foundation for several investigations of severe thunderstorms (Fujita 1982; Fujita and Dodge 1983; Mack et al. 1983), hurricanes (Mack et al. 1983; Rodgers et al. 1983), and cloud emissivity (Szejwach et al. 1983) that demonstrate the importance of stereo imagery as a diagnostic tool for satellite meteorology and cloud remote sensing. However, considerable human effort and interpretation was required to retrieve these height estimates, and it was not until the advent of multiprocessor computer systems and the work of Hasler et al. (1991) that this process was largely automated. Today much more powerful computer systems are available yet with the exception of Wylie et al. (1998) and Mahani et al. (2000), the use of GOES satellites for stereo imaging experiments has received limited attention and has utilized only visible wavelength channels.

In recent years several instrument payloads providing multiangle measurement capabilities have been placed in low earth orbit. Two examples are the along-track scanning radiometer (ATSR and ATSR-2) and the multiangle imaging spectroradiometer (MISR). The ATSR and ATSR-2 instruments, launched in 1991 and 1995, respectively, are spin-scan radiometers that acquire imagery in four spectral channels including both shortwave and thermal infrared wavelengths (Prata et al. 1990). These data provide diurnally unbiased estimates of cloud-top heights and cloud motion winds (Lorenz 1985; Prata and Turner 1997). The multiangle imaging spectroradiometer was launched aboard the *Terra* spacecraft in 1999 and consists of nine push broom radiometers pointing both fore and aft (Diner et al. 1998). Each radiometer includes four linear array detectors and acquires data in spectral channels ranging from the blue to the near-IR. As such, the MISR instrument can provide stereoscopic estimates of cloud-top heights and cloud motion winds, but the choice of spectral channels restricts these measurements once again to sunlit conditions only (Horvath and Davies 2001).

The current work reports upon stereo cloud height measurements made using the infrared spectral imaging radiometer (ISIR) during mission STS-85 of the space shuttle *Columbia.* The ISIR instrument is a push broom radiometer that was the first among earth and climate imaging systems to employ an uncooled microbolometer array detector to acquire thermal infrared measurements. Although it was not designed specifically to provide stereo cloud height estimates, use of this extended array makes such measurements readily available. The goal of this paper is to evaluate the utility of the ISIR instrument design and the microbolometer detector technology as the basis of an operational cloud stereo imaging system. This begins with a description of the instrument and the measurements that were made using it. Sample stereo results are presented and the resulting cloud height estimates are compared to ranging data obtained simultaneously with the shuttle laser altimeter (SLA; Bufton 1989; Garvin et al. 1998). The paper concludes with a discussion of these results within the context of the requirements of an operational, infrared stereo imaging system.

2. Instrument and experiment description

The infrared spectral imaging radiometer was developed by NASA Goddard Space Flight Center and Space Instruments Incorporated around an uncooled microbolometer array detector for the purpose of assessing the potential of this technology as an imaging sensor for small satellite missions. The advantage offered by this type of detector is that the resulting instrument payload can be made both compact and lightweight since there is no need for aggressive cooling. This absence of a cooler is also the reason a large commercial market has developed for these devices in law enforcement and fire fighting. The ISIR instrument is a push broom imager that includes four spectral channels, three of which have 1-μm passbands and are centered at wavelengths of 8.6, 10.2, and 11.8 μm. A fourth channel measures broadband radiation covering the spectral region of 7–13 μm. The spatial resolution of the acquired imagery is approximately 250 m with a swath of 90 km when operated from shuttle orbit.

A primary objective in the development of the ISIR instrument was to arrive at a compact design that could be easily accommodated within a shuttle hitchhiker vessel known as a Get Away Special can. Shown in Fig. 1 is the resulting instrument design, which includes an optics module, an electronics module, and a calibration assembly. Also included within the instrument is an onboard blackbody source whose temperature is controlled using a stack of thermoelectric coolers. This source is mounted outside of the optical axis and periodically a moveable calibration assembly is positioned such that an unfocused image of the source is projected through the imaging lens and onto the focal plane. This calibration arm remains outside of the optical path when acquiring imagery of the earth.

The optics module is composed of a multielement lens system, four spectral filters, and the infrared detector package. The lens assembly images directly onto the focal plane with a speed of F/0.8 and is optimized for operation in the 8–14-μm wavelength region. The

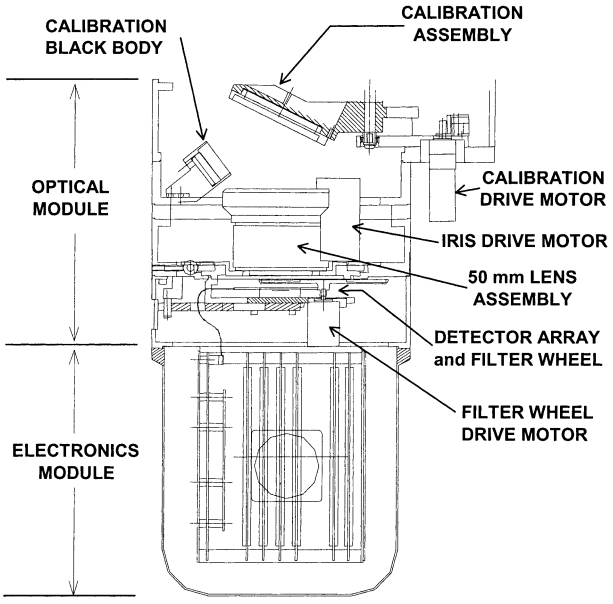

FIG. 1. The ISIR was included among the complement of Hitchhiker instruments aboard mission STS-85. Operating from the space shuttle *Columbia*, the ISIR instrument was the first space-borne cloud radiometer built around an uncooled microbolometer array detector.

spectral filters are 1 in. in diameter and are composed of several multilayer interference coatings deposited upon Ge/ZnSe substrates. Each is mounted within a filter wheel positioned directly above the detector focal plane. A complete cycle of the four filters requires approximately 6.67 s; a period dictated by the requirement for contiguous imagery and made necessary by the shuttle altitude. The electronics module houses eight printed circuit boards that control the operation of and communication with the camera. The ISIR instrument also includes two large-capacity, 8-mm tape drives capable of storing 14 GBytes of data when compressed at an average 2:1 compression ratio. These tape drives are not shown in Fig. 1.

The uncooled infrared array detector incorporated into the ISIR instrument is an early prototype model manufactured by Lockheed Martin Infrared Systems. It provides a format of 327 $\times$ 246 pixels that are each 46.25 μm in size. The array is mounted within a housing package that is covered with a thin germanium window and sealed hermetically. This package is integrated onto a front-end focal plane board that provides the readout electronics. Also included in this imaging module are a video signal processing and controller electronics card, and a power supply card. The imaging module provides a rolling readout of the detector array with 14-bit precision at a rate of 60 frames per second.

When coupled with the forward motion of the space shuttle use of this extended array detector makes possible a frame averaging technique known as time delay and integration (TDI). Using this technique the signal-to-noise ratio (S/N) of the acquired imagery is improved by integrating successive rows of detectors in a time-delayed sequence, adding the signals from pixel elements originating at the same earth location. This approach requires that the readout of the camera be synchronized with the forward motion of the orbiting platform. Given the design of the ISIR optics and the limitations of the detector electronics, the required synchronization (30 fps) was optimal at an orbital altitude of 140 n mi. The shuttle operated at an altitude of approximately 160 n mi for most of mission STS-85. During this time imagery was acquired, but with fractional pixel blur. On day 10 a burn of the main thruster was performed to reduce the altitude to accommodate high-resolution imagery by the ISIR experiment for the last 2 days of the mission.

The use of TDI necessarily imposes constraints upon the attitude of the orbiting platform, the severity of which depends upon the number of successive rows desired in the time delay and integration average. For ease of computation the forward motion of the platform was restricted to one dimension of the detector array. Doing so simplifies considerably the relative registration of the imagery and allows for precise timing of the detector readout. The rotation of the earth, however, presents a challenge to maintaining this alignment as its contribution to the scene velocity varies with latitude. To obtain the highest pixel resolution, it is necessary to continually slew the instrument yaw to counter this effect and maintain the desired alignment. In the measurements of the current work the attitude thrusters of the shuttle provided these necessary slew adjustments.

During the majority of mission STS-85 the shuttle orientation was maintained relative to the ground velocity vector with a precision of 0.5°. Upon reducing the orbital altitude to 140 n mi, the shuttle was operated in a special low cross-track motion steering mode. This provided a precision of 0.1° relative to the ground velocity vector. At the higher orbital altitude 10 rows were included in the TDI average. While at an altitude of 140 n mi the size of the TDI average was increased to include 40 rows. In the latter case the cross-row drift did not exceed 1/8 pixel during the time required to accomplish the TDI average. The orientation of the detector array relative to the shuttle was set prior to launch, after receipt of the flight plan.

3. Stereo retrieval methodology

Stereoscopic retrieval of cloud height requires that each scene be viewed from two perspectives. This can be accomplished either by using two separate instruments to view a common scene simultaneously or a single instrument to view each scene sequentially from two locations. Both techniques present observational challenges. The use of multiple instruments requires that the analysis contend with differences in instrument design, and unless they are flown in formation stereo imagery will be limited to only those times of coincidental

pointing. The challenge presented by use of a single instrument is that the two perspectives must be acquired before the cloud scene changes appreciably. Fundamental to the design of the ISIR instrument is the concept of viewing the same scene sequentially from multiple locations.

The extended infrared array detector of ISIR is used to acquire imagery over an approximate $16.8° \times 10.4°$ instantaneous field of view with the long dimension oriented in the cross-track direction. Due to the motion of the shuttle this imagery appears to be in continual motion with features entering on one side and exiting on the opposing side. Radiometric samples are obtained sequentially using each of the four spectral filters before the scene has sufficient time to pass and thus encoded in the imagery of the spectral channels are different perspectives. A comparison of these spectral data reveals features at different altitudes appearing to move relative to one another as a result of parallax. Quantifying this apparent motion provides the necessary mechanism to retrieving the altitude information.

This quantification begins by locating common features in the imagery from a pair of spectral channels. In doing so one of the images is defined to be the ''reference image'' and the other to be the ''search image.'' The reference image is divided into a regular grid of smaller subimages, or ''patches,'' that are compared to identically sized areas within a select window of the search image. With each comparison a value of χ^2, defined as

$$\chi^2 = \frac{1}{N} \sum (y_i - x_i)^2,$$

where x_i and y_i are the values of the ith pixel within the reference and search image patches and N is the number of pixels included in the patch region, is calculated. The average values of x and y for a select patch are subtracted from x_i and y_i prior to calculating χ^2 to account for differences in the absolute brightness of different patches. The best match is assumed to be found when χ^2 is at a minimum. There is no threshold for acceptance of χ^2 and a minimum of two pixels is needed to define the brightness variation that makes up a patch with the presence of noise increasing this requirement.

The combination of spacecraft motion, speed of the imaging optics, and the elapsed time between images dictate the location of the window that is examined in the search image. Additionally, knowledge of the spacecraft altitude combined with the detector pixel size provides an estimate of the area this window must encompass to accommodate parallax values typical of cloud altitudes. Each pixel in the imagery of the current work represents approximately 2 km of vertical motion due to parallax and clouds tend to be located at altitudes less than about 10 km. Thus the size of the window in the search image is conservatively set at ± 5 pixels larger than the selected patch in the reference image to allow for apparent translation due to parallax. The search for the match is restricted to one dimension of the image as the shuttle attitude was controlled to limit the amount of cross-track motion to less than a single pixel.

Upon finding the best match the determined value of ''displacement'' is recorded for that region of the image and the search algorithm advances to operate on the subimage contained within the next grid location. The optimal size of the patches that make up this grid is not known a priori. As the horizontal resolution of the stereo results is dependent upon this grid, it is desirous that it be composed of patches that include a small number of pixels. However, the patches must also include a sufficiently large number of pixels that a high correlation probability results. In the current work the adopted approach is to run the pattern-matching algorithm using several choices of grid resolution, thereby providing several estimates of displacement for each pixel, from which an average is calculated. The highest resolution grid that is employed consists of 3×3 pixel regions and the lowest resolution grid is made up of patches that are 22×22 pixels in size.

The uncooled infrared array detector used in the ISIR instrument is an early prototype model that exhibits a considerable amount of fixed pattern noise. The majority of this noise is removed through frequent calibrations. However, for regions of an image showing little variation in brightness a high probability remains that the pattern-matching algorithm will search out the residual noise pattern rather than the select cloud feature. When this occurs the registration of a pixel is erroneous and the search algorithm returns identical estimates of displacement regardless of the grid resolution that is used. When not dominated by fixed pattern noise, the search algorithm returns estimates of displacement exhibiting a statistical variation for each pixel. Those pixels that do not exhibit at least a 5% scatter in the determined displacements among the different grid resolutions are discarded, and the remaining irregular grid of values are used in the construction of a Delaunay triangulation. The results of this triangulation are then used to interpolate the cloud heights to the original regular grid using a linear quintic polynomial.

After the average displacement has been calculated for each pixel, a correction is applied to normalize the results to that of the nadir pixel. Even though each pixel shares a common angular IFOV, the nadir pixel represents the smallest footprint and those pixels at the edges of the detector represent the largest. As a result, features sharing a common altitude translate across the image at different rates depending upon their location on the detector. The rate of translation is greatest across those pixels representing smaller footprints. Without this correction stereo cloud heights are underestimated for pixels that are not at the center of the array. The top panel of Fig. 2 illustrates the sinusoidal variation of the footprint across the image and the bottom panel shows the corresponding correction that must be applied to the

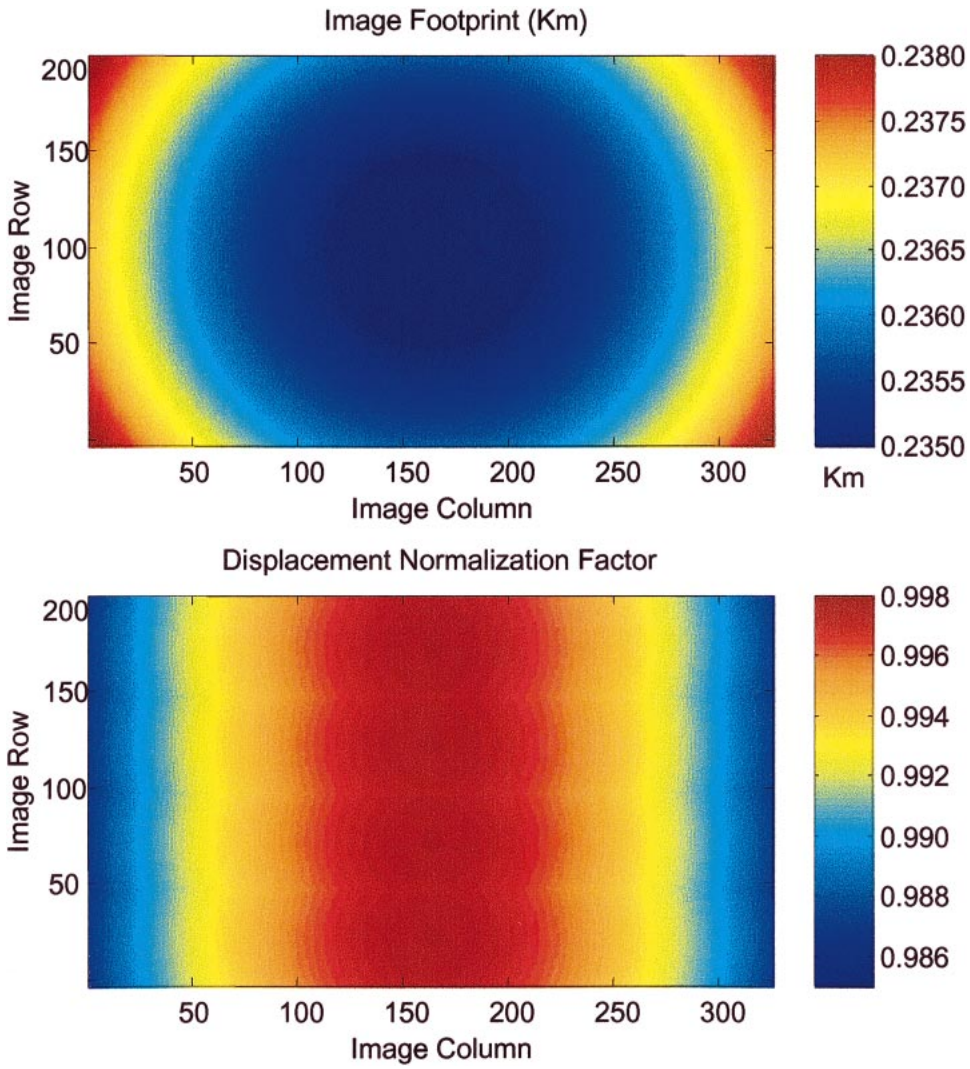

FIG. 2. Each pixel of the ISIR instrument shares a common angular IFOV and the corresponding footprint follows (top) a cosine variation about the nadir pixel. As a result a (bottom) correction factor must be applied to the cloud height estimates to remove this dependence.

values of pixel displacement. These results were modeled using the measured value of 903 $\pm$ 3 μrad for the IFOV.

The normalizing coefficient shown in the lower panel of Fig. 2 is repeated 4 times within an image. This banding is illustrative of the manner in which the spectral channels are combined to provide contiguous stereo results. Four filters were cycled in front of the detector array to provide multispectral imagery. Due to the forward motion of the shuttle the scene moves roughly one-fourth of the way across the image in the time allotted to a single channel. The imagery obtained in any two consecutive channels thus contains overlapping scene information for approximately three-fourths of the image, albeit from slightly different perspectives. The stereo analysis is performed using those spectral channel pairs that have only one-fourth of an image in common, with the common imagery appearing at opposing sides of the detector array. It is in this circumstance that the maximum 7.8° change in perspective is achieved.

The data displayed in Fig. 2 are model results, and in practice it is more reliable to apply a correction that has been determined experimentally using imagery of broken, single-altitude cloud layers that are nearby in the orbit. The requisite broken cloud imagery is easily identifiable as the attendant clouds exhibit a largely uniform brightness in the infrared. An example of an experimentally determined correction is shown in Fig. 3. Surface imagery can also be used in some cases. However, as ISIR was not optimally designed for surface measurements the preferred approach is one of using cloud scenes. It should be noted that the imagery from all four spectral channels is required to obtain contiguous stereo results.

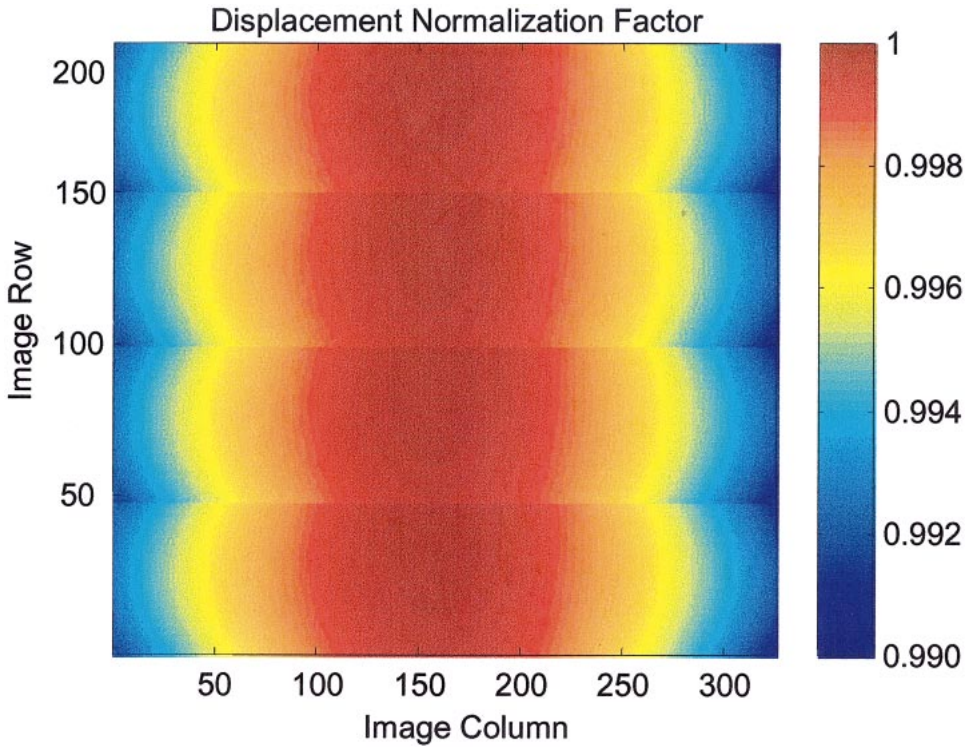

FIG. 3. Same as the bottom panel of Fig. 2 except that the correction factor is determined experimentally from select cloud imagery.

4. Measurements

During mission STS-85 nearly 60 h of multispectral imagery was collected with the ISIR instrument over a period of 10 days. The retrieval algorithm described above has been applied to select portions of these data and the results of three representative cases are chosen for presentation. These cases are selected with the goals of demonstrating 1) the feasibility of the stereo retrieval algorithm, 2) the accuracy of the stereo height retrievals, and 3) the vertical precision with which the height estimates are achieved. The following is arranged such that Figs. 4, 5, and 6 address each of these goals in turn with the latter two utilizing a comparison of results from direct detection ranging using the SLA.

The feasibility of the stereo retrieval algorithm is illustrated by the results of Fig. 4 wherein imagery of a cloud scene that exhibits well-defined features is presented. These data represent an approximate 18-s segment of data and are a compilation of three individual frames. The forward motion of the shuttle is in the long dimension of the image and the aspect ratio matches that of the camera. The panel on the left contains a false-color image of the radiance as measured through the 10.2-μm channel of the instrument. The panel on the right contains the corresponding cloud-top heights that were retrieved using the stereo algorithm described above. This imagery is particularly useful as a first test of the stereo retrieval algorithm as the strong cloud features at several different altitudes readily facilitate qualitative confirmation of the stereo results. Various cloud layers are revealed including low-level cumulus clouds at an altitude around 1.5 km, midlevel clouds near 5 km, and an aged contrail reaching as high as 8 km.

When viewed in the image of calibrated radiance the midlevel cloud near 5 km, located in the upper right-hand corner of the images of Fig. 4, appears to be a possible mixture of semitransparent clouds at different altitudes. Such cloud layers present an obstacle to the accurate retrieval of height using stereo techniques and the utility of this method is often reduced as a consequence. The reason being that the blend of partially transmitting layers makes pattern matching difficult and less well defined. This is also the case for portions of the contrail that are thin as they transmit IR radiation from below. The stereo technique implemented here uses a simple pattern-matching algorithm with a limited ability to distinguish partially transmitting clouds. As such, features of the top surface of the cloud can be hard to distinguish and lower cloud heights can be returned as a result.

During mission STS-85 the shuttle *Columbia* became the first space-based platform to combine laser ranging and thermal IR cloud remote-sensing payloads. The resulting combined dataset is thus unique in satellite meteorology providing an unprecedented opportunity to validate the stereo results through a comparison with

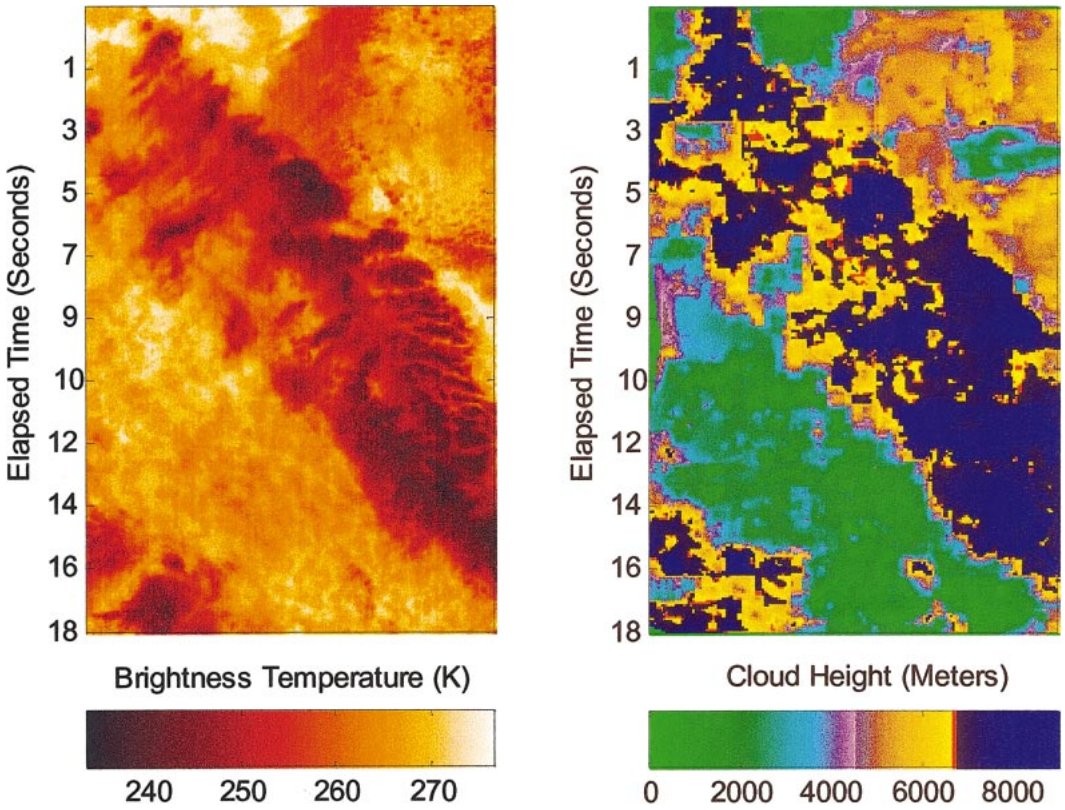

FIG. 4. (left) A sample of the radiometric imagery obtained with the ISIR instrument during mission STS-85. (right) The corresponding estimates of cloud height obtained using stereoscopic techniques. A multilayered cloud system is seen that includes an aged contrail at an altitude near 8 km.

direct detection measurements. Additionally, the high precision lidar measurements can be used to quantify the variability inherent to the cloud top, thereby removing the ambiguity between this variability and the vertical precision of the stereo measurement. Prior to launch the ISIR instrument was aligned to the Shuttle Laser Altimeter so that a direct comparison of the two measurement techniques could be made. The SLA was designed to collect surface altimetry and was not optimized for cloud detection or profiling. Still, the data that were collected routinely contain height information on cloud tops that provide meaningful comparisons with the ISIR stereo results.

To validate the accuracy of the stereo retrieval algorithm against the SLA data an optically thick cloud scene that results in strong lidar returns and which spans a wide range of altitudes is optimal. A quantitative comparison between the ISIR stereo and SLA direct detection results can be achieved by restricting the retrieved stereo cloud heights to only those that share a common field of view. Such a comparison is shown in Fig. 5 where the solid line represents the results of the stereo retrieval and the diamonds represent the measurements of the SLA instrument. As expected the stereo results show a much higher degree of scatter than do the direct detection lidar measurements. However, the two instruments are clearly measuring the same cloud region and obtaining results that agree favorably. A notable exception to this conclusion is seen in the data indexed near 30 s, where the cloud is shown by the lidar measurements to be multilayered with surfaces at 4 and 6 km. The scale of this horizontal structure is too fine to be retained by the stereo algorithm and it appears that the pattern-matching algorithm may be focusing disproportionately on the cooler features.

The stereo cloud height estimates of Fig. 5 are restricted to only those pixels that coincide with the ground track of the SLA. It should be noted, however, that while the footprint of the SLA instrument is contained within a single pixel of the infrared image, an extended region of pixels is required to arrive at a stereo height estimate. In the current work, image features located up to 11 pixels from the pixel to which the result is assigned influence each height estimate. This should be recognized when interpreting the results of the stereo height calculations on the scale of a single pixel. In addition, pixels located within regions displaying insufficient structure to accommodate the pattern recognition algorithm are assigned height estimates based upon the results of nearby pixels. Thus, uniform regions of an image can be neglected and assigned the height of a nearby cloud layer.

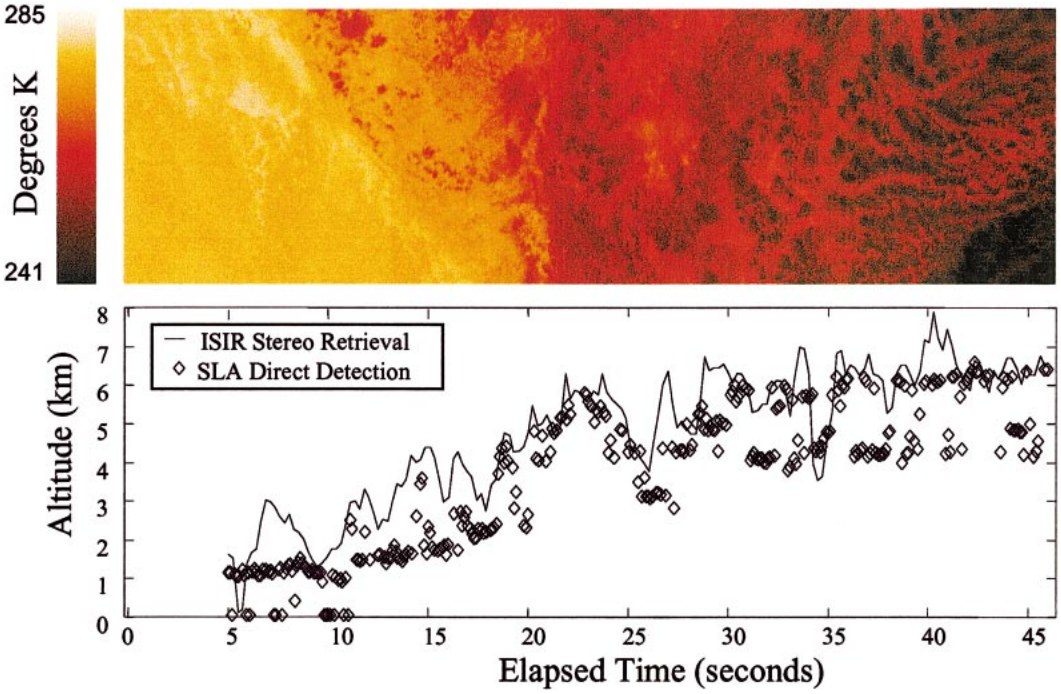

FIG. 5. Prior to launch the ISIR instrument was aligned with the SLA to facilitate a comparison of the measurements provided by the two instruments. Shown here is a comparison of cloud height estimates obtained using stereoscopic techniques and through direct detection for an optically thick cloud scene that reaches as high as 6-km altitude.

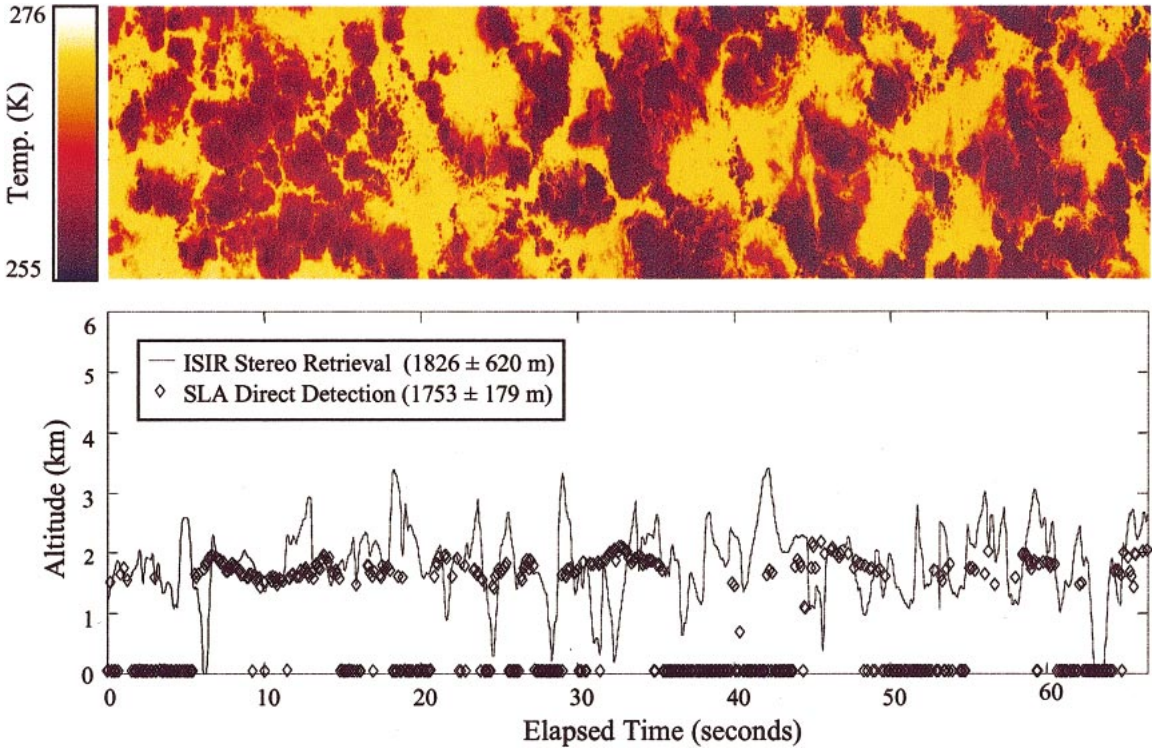

FIG. 6. A scene of broken cumulus clouds is used to estimate the vertical resolution of the stereoscopic cloud height measurements by comparing them with direct-detection measurements from the SLA. Inversion of the ISIR stereo imagery results in an average cloud height of 1826 ± 620 m, whereas the direct detection measurements of the SLA reveal an average height of 1753 ± 179 m.

The results of Fig. 6 are used to provide an estimate of the vertical resolution that is achieved with the ISIR stereo measurements. Here the solid curve represents the stereo measurements and the diamonds represent the direct-detection measurements. The direct-detection measurements reveal the average height of the cloud tops to be at 1753 ± 179 m. The uncertainty in this value is primarily the result of variations in cloud-top altitude and is not representative of the precision of the direct-detection measurement. The stereo measurements reveal the cumulus clouds to be located at an average altitude of 1826 ± 620 m. This standard deviation is a measure of the vertical precision achieved by the stereo observations as the variability of the cloud tops, revealed through the SLA instrument, is small by comparison. Although this precision estimate tends to vary somewhat according to the chosen imagery, ±620 m is representative of the vertical height resolution achieved for a single pixel of the ISIR imagery.

The use of laser profiling to define cloud heights is well known for airborne and ground-based applications. These cloud lidar systems are designed to record an entire profile of the return signal, up to the signal attenuation limit (Spinhirne et al. 1982). As such they provide measurements of both the upper and lower cloud boundaries and a profile of the interior of those clouds that present an optical depth less than unity. For optically thick clouds a region of penetration is sampled and typically the strongest signal is returned from several hundred meters within the cloud, when viewing in the nadir.

The SLA data system was not designed to accomplish this measurement but rather to trigger offset signal levels, recording a small portion of the signal immediately prior to and just after the trigger threshold events. Due to the design of SLA and various noise considerations the trigger threshold was set high relative to signals from cloud tops. Consequently, less dense clouds such as thin cirrus were generally not detected. For those cloud cases where a trigger was obtained the threshold detection could be as much as kilometers below the higher thin layers of the cloud top. For the more uniform status clouds of Fig. 5, and those of Fig. 6 that show a consistent detection of the layer, aircraft lidar experience would indicate a true cloud top within a few hundred meters of the detected threshold altitude.

5. Discussion

Multiangle remote sensing provides several opportunities for advancing current understanding of geophysical and biophysical parameters (Diner et al. 1999). Recent instruments placed in low earth orbit such as ATSR and MISR have been developed specifically for this purpose. Additionally, the network of geosynchronous weather satellites can contribute limited multiangle observations, albeit with considerable effort as they currently are not designed to operate in a manner that easily accommodates the requisite synchronization. As the scientific issues that require multiangle observations are both rich and diverse additional instrumentation will be required in the future. It is the designs of these instruments that can benefit from the continued advancement of technology offering the potential of greater versatility contained within a design that is more compact and robust.

The infrared spectral imaging radiometer was the first earth remote-sensing instrument to incorporate an uncooled microbolometer array detector as its image sensor. Its relatively simple camera design is conducive to providing reliable, operational multiangle imagery. Hence, the potential is great that the ISIR instrument, or a minor variant thereof, can provide a powerful multiangle, remote-sensing tool for satellite meteorology. The current work illustrates this multiangle capability through the stereo inversion of cloud-top height. In the discussion that follows three aspects of the ISIR operation and performance are addressed: 1) the achieved vertical height resolution, 2) the optimization of the stereo retrieval algorithm, and 3) the possibility of measuring winds simultaneously with cloud heights.

The vertical height resolution of the current work was estimated by comparing stereo measurements with height estimates obtained simultaneously through direct detection using the Shuttle Laser Altimeter. As mission STS-85 was the first to overcome the challenges of including both the laser ranging and stereo imaging systems on the same space platform, previous investigators were left to rely upon other characterizations of measurement precision as shown in Table 1. As is evident by the dearth of case data, obtaining an empirical verification of vertical resolution is an elusive task. The resolution of the *Apollo 6* measurements of Whitehead et al. (1969) and Shenk et al. (1975) were estimated by independently assessing the extent of the shadows cast by the clouds themselves. The investigations of Minzner et al. (1978), Hasler (1981), and Prata and Turner (1997) sought out stereo imagery of terrestrial features such as mountains and lakes of known elevation for comparison. These features are, however, both extended and well defined and as such their suitability for characterizing the resolution of a cloud measurement is less than ideal.

It is also seen in Table 1 that the current design of ISIR provides a vertical resolution similar to those of previous instruments thereby meeting the requirements typical of past stereo cloud investigations. This achieved resolution of ±620 m corresponds to a single pixel of the ISIR image and the average cloud height can be identified with considerably more precision by averaging the single pixel results. This is illustrated in Fig. 7 using imagery from the broken cumulus layer of Fig. 6. Coincident measurements of the SLA show the variability of this cloud layer to be approximately ±180 m. The precision of the stereo measurements in Fig. 7 asymptotically approaches this value when the bin size

Table 1. An empirical determination of the achieved vertical resolution requires an independent measure of height to which the stereo estimates can be compared. Shown here are the published estimates of previous investigators and the methods that were used to arrive at these estimates.

Stereo measurement	Platform	Vertical resolution	Verification
Whitehead et al., (1969) Shenk et al. (1975)	*Apollo 6*	±0.5 km	Cloud shadows
Minzner et al. (1978)	GEO, separated by 32° lon	Approx. ±0.3 km	16 mountain features, 1 lake
Hasler (1981)	GEO, separated by 60° lon	Approx. ±0.5 km	Coastlines, mountain lakes
Prata and Turner (1997)	Low earth orbit	±1 km	Mountain topography
Current work	Space shuttle	±0.6 km	Simultaneous cloud laser ranging

reaches about 150 × 150 pixels representing a 38 km × 38 km area.

The optical design of ISIR provides a maximum parallax angle of approximately 7.8° and a spatial resolution of about 0.25 km when in shuttle orbit. Using these values it is straightforward to calculate that a single pixel of parallax represents roughly a 1.8-km change in altitude. This approximate agreement with the experimentally determined vertical resolution lends support to the credibility of the stereo inversion algorithm, and, in particular, the image registration technique that searches out matching regions of the reference and search images. As stated, the current work divides the referenced image into a grid of smaller subimages or patches that are registered to a search image. Several factors necessarily influence the optimal choice of resolution for this grid. Choosing a grid that is too coarse will reduce the vertical resolution of the stereo results, as neighboring cloud features will not be sufficiently resolved. Choosing a grid that is too fine will also reduce the vertical resolution since the detector noise will impact the results disproportionately.

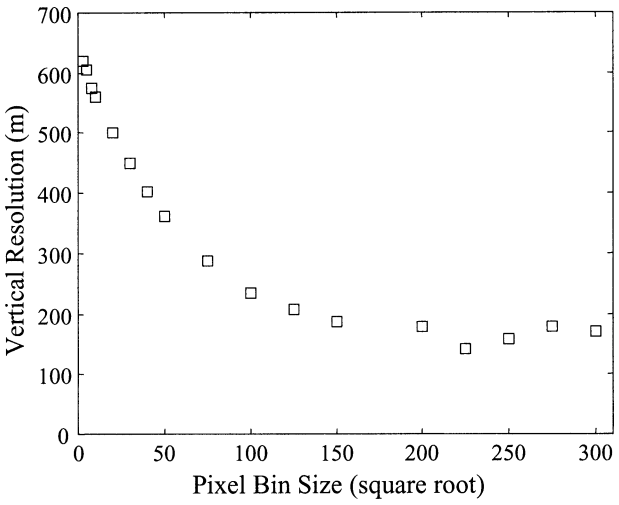

FIG. 7. The average height of a cloud layer can be determined more precisely than that of a single pixel by binning the stereo results. This is demonstrated here by binning the results of the data in the previous figure. The asymptotic precision of the stereo results is seen to be approximately ±180 m for this cloud layer, in agreement with the cloud-top variability measurements of the SLA.

The optimal choice of grid resolution can be gleaned by correlating the stereo height returns for different selections of resolution with the image brightness temperatures. Clouds tend to be in near–thermal equilibrium with the surrounding atmosphere and thus cooler cloud features are seen at higher altitudes and warmer ones at lower altitudes. Thus the optimal grid resolution is that which results in the greatest correlation between these two. This approach to evaluating the optimal grid resolution does have shortcomings as a cloud is not a perfect blackbody and a thin cloud will exhibit an elevated brightness temperature as it transmits much of the radiation from the warm surface below. Thus, the correlation will not be exact but should give an indication of the optimal choice of grid for use in the search algorithm. This lack of perfect correlation is in itself an argument for using stereoscopic inversion methods to determined cloud height.

Shown in Fig. 8 are results from a correlation study that uses the imagery of the contrail scene shown in Fig. 4. The correlation between cloud height and brightness temperature appears to maximize when the reference image is divided into patches that are composed of 70–100 pixels, with a 100-pixel region representing a 10 × 10 pixel grid resolution. The maximum of the correlation coefficient is not sharp and a host of patch sizes ranging from 8 × 8 pixels to 16 × 16 pixels provide similar results. The current work uses selections of grid resolution ranging from 3 × 3 pixels to 22 × 22 pixels and the correlation results of Fig. 8 are used as a weighting function when computing the average of the results from the different grid choices. That the correlation is not optimal for a 3 × 3-pixel grid resolution is a reflection of the detector noise limitations, as it is not unusual for the stereo results of as many as one-fourth of the pixels to be discarded and replaced through interpolation. Current production detectors offer greatly reduced fixed pattern noise and factor of 2 improvements in radiometric performance.

A primary reason to measure cloud height is to enable the assignment of wind speed when observing cloud motions apparent in a time series of satellite images.

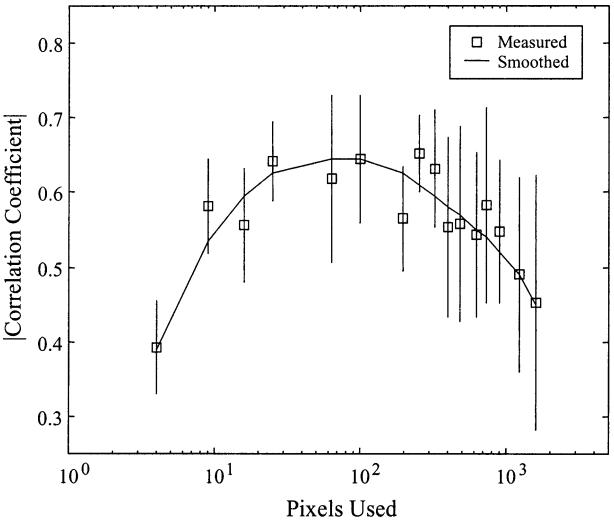

FIG. 8. The correlation between cloud height and brightness temperature provides a means to determine the optimal grid resolution used in the search algorithm of the ISIR imagery. Using the imagery of Fig. 4 it is seen that an approximate 10×10 pixel grid provides the best correlation between the brightness temperature and stereoscopic cloud height. These results are used to weight the average of stereo height estimates obtained using different grid resolutions.

Winds gleaned in this manner are known as cloud motion winds, and it is the independent measure of cloud height that provides the needed calibration for this measurement. One approach to achieving this is to couple a laser ranging system with a single stereo camera. The laser ranging system provides the requisite independent measure of cloud height that is used together with the stereo imagery to glean estimates of cloud motion that occurred as a result of wind.

The measurements of the current work are made using this combination of instruments. The ISIR instrument, however, was not ideally configured for this measurement as less than 6.7 s elapsed between the acquisition of the images that make up the stereo pair. With a spatial resolution of approximately 0.25 km, a single pixel of motion represents a wind speed in excess of 37 m s^{-1}. As such, the stereo retrievals that result from the ISIR design are seen to be largely insensitive to typical cloud motions. This lack of sensitivity makes the height measurements of the Shuttle Laser Altimeter particularly useful in calibrating the stereo height retrievals. However, the combined stereo and laser ranging measurements are not particularly useful for retrieving wind estimates.

6. Conclusions

The ISIR instrument is unique among thermal imaging systems developed for use in satellite meteorology being the only one thus far to incorporate an uncooled microbolometer array detector as its image sensor. Because the development of this detector technology is relatively recent considerable uncertainty remains regarding its potential for satisfying the demands of infrared earth and climate monitoring systems. However, it is through pilot experiments such as the one reported here that this potential can be assessed. The focus of the current work is upon the possibility of using this detector technology in the development of an operational stereo cloud remote-sensing instrument. Toward that end, a stereo algorithm was developed to retrieve estimates of cloud-top height from the multispectral imagery collected with this sensor during the STS-85 mission of the space shuttle *Columbia*. Cloud-top heights were measured with a resolution of approximately ± 620 m in good agreement with that anticipated from the optical design. A comparison with direct detection measurements of the Shuttle Laser Altimeter confirms the accuracy of the stereo retrievals.

The ISIR program was designed to generally address the potential of the microbolometer detector array as a space sensor and not specifically to develop a cloud stereo imaging system, even though the current work examines the possibility of using this device for this specific purpose. When placed on board a spacecraft in low earth orbit rather than on the shuttle, the vertical height resolution offered by the ISIR design would be reduced by about a factor of 2. Hence, to retain the vertical precision either the spatial resolution would need to be increased at the expense of the FOV or a larger format than the 327×246 pixel array would need to be implemented. Uncooled microbolometer array technology has advanced considerably since the ISIR instrument was built and flown. Today, microbolometer detector arrays are readily available in formats of 640×480 pixels. Further, only modest technical challenges need to be overcome to produce arrays with formats of 1024×1024 or larger. The primary hurdle to developing this format is the emergence of a commercial market that demands such a product.

In developing an operational stereo imaging system based upon the ISIR design a potential modification would be to eliminate the narrow band spectral filters. If the objective of the measurement is solely stereo retrieval then there is little reason not to utilize the full spectral response of the detector to maximize the S/N of the imagery. In this way the instrument can be made very small with sizes comparable to that of head-mounted, military thermal cameras. An instrument of this size could easily be accommodated by a host of satellite platforms. This smaller size also makes possible the use of multiple cameras each pointing in different directions instead of the stereo imaging being performed using only a single detector as with ISIR. Similarly, compact stereo instruments could be flown in formation on a constellation of small satellites. Using this approach it would be possible to measure atmospheric winds as well by observing the amount of cloud motion that takes place in the intervening time between the passage of the two stereo cameras.

Last, these measurements provide a good pilot experiment for future satellite meteorology missions that combine infrared stereo imagery and direct-detection lidar. Combined measurements of this sort would, however, benefit from a lidar system that is able to provide a cloud profile rather than merely range altitude. Such a system would provide information about the thickness of a cloud system and the presence of multiple cloud layers; characteristics important to accurately model cloud microphysical properties. The first operational space-borne lidar missions are planned for the next few years (Spinhirne and Palm 1996), but current constraints limit sampling to the nadir for the foreseeable future. Coupling an infrared stereo imaging instrument such as ISIR with these planned missions would provide a unique opportunity to extend the spatial coverage beyond that sampled directly by the lidar and to improve the accuracy and understanding of the passive observations.

Acknowledgments. The authors would like to acknowledge the support of the NASA Radiation Sciences Program and the Goddard Shuttle Small Payloads Office.

REFERENCES

Bristor, C. L., and W. Pichel, 1974: 3-D cloud viewing using overlapped pictures from two geostationary satellites. *Bull. Amer. Meteor. Soc.,* **55,** 1353–1355.

Bufton, J. L., 1989: Laser altimetry measurements from aircraft and spacecraft. *Proc. IEEE,* **77,** 463–477.

Diner, J. D., and Coauthors, 1998: Multi-angle imaging spectroradiometer (MISR) instrument description and experiment overview. *IEEE Trans. Geosci. Remote Sens.,* **36,** 1072–1085.

——, and Coauthors, 1999: New directions in Earth observing: Scientific applications of multiangle remote sensing. *Bull. Amer. Meteor. Soc.,* **80,** 2209–2228.

Fujita, T. T., 1982: Principle of stereoscopic height computations and their applications to stratospheric cirrus over severe thunderstorms. *J. Meteor. Soc. Japan,* **60,** 355–368.

——, and J. C. Dodge, 1983: Applications of stereoscopic height computations from dual geosynchronous satellite data/joint NASA–Japan stereo project. *Adv. Space Res.,* **2,** 153–160.

Garvin, J., J. Bufton, J. Blair, D. Harding, S. Luthcke, J. Frawley, and D. D. Rowlands, 1998: Observations of the Earth's topography from the Shuttle Laser Altimeter (SLA): Laser-pulse echo-recovery measurements of terrestrial surfaces. *Phys. Chem. Earth,* **23,** 1053–1068.

Hasler, A. F., 1981: Stereographic observations from geosynchronous satellites: An important new tool for the atmospheric sciences. *Bull. Amer. Meteor. Soc.,* **62,** 194–212.

——, R. Mack, and A. Negri, 1983: Stereoscopic observations from meteorological satellites. *Adv. Space Res.,* **2,** 105–113.

——, J. Strong, R. H. Woodward, and H. Pierce, 1991: Automatic analysis of stereoscopic satellite image pairs for determination of cloud-top height and structure. *J. Appl. Meteor.,* **30,** 257–281.

Horvath, A., and R. Davies, 2001: Feasibility and error analysis of cloud motion wind extraction from near-simultaneous multiangle MISR measurements. *J. Atmos. Oceanic Technol.,* **18,** 591–608.

Kikuchi, K., and T. Kasai, 1968: Stereoscopic analysis of photographs taken by NIMBUS II APT system. *J. Meteor. Soc. Japan,* **46,** 60–67.

Lorenz, D., 1985: On the feasibility of cloud stereoscopy and wind determination with the Along-Track Scanning Radiometer. *Int. J. Remote Sens.,* **6,** 1445–1461.

Mack, R., A. F. Hasler, and E. B. Rodgers, 1983: Stereoscopic observations of hurricanes and tornadic thunderstorms from geosynchronous satellites. *Adv. Space Res.,* **2,** 143–151.

Mahani, S. E., X. Gao, S. Sorooshian, and B. Imam, 2000: Estimating cloud top height and spatial displacement from scan-synchronous GOES images using simplified IR-based stereoscopic analysis. *J. Geophys. Res.,* **105,** 15 597–15 608.

Minzner, R. A., W. E. Shenk, R. D. Teagle, and J. Steranka, 1978: Stereographic cloud heights from imagery of SMS/GOES satellites. *Geophys. Res. Lett.,* **5,** 21–24.

Nieman, S. J., J. Schmetz, and W. P. Menzel, 1993: A comparison of several techniques to assign heights to cloud tracers. *J. Appl. Meteor.,* **32,** 1559–1568.

Ondrejka, R. J., and J. H. Conover, 1966: Note on the stereo interpretation of Nimbus II APT photography. *Mon. Wea. Rev.,* **94,** 611–614.

Prata, A. J., and P. J. Turner, 1997: Cloud-top height determination using ATSR data. *Remote Sens. Environ.,* **59,** 1–13.

——, R. P. Cechet, I. J. Barton, and D. T. Llewellyn-Jones, 1990: The Along-Track Scanning Radiometer for *ERS-1*—Scan geometry and data simulation. *IEEE Trans. Geosci. Remote Sens.,* **28,** 3–13.

Rodgers, E. B., R. Mack, and A. F. Hasler, 1983: A satellite stereoscopic technique to estimate tropical cyclone intensity. *Mon. Wea. Rev.,* **111,** 1599–1610.

Shenk, W. E., R. J. Holub, and R. A. Neff, 1975: Stereographic cloud analysis from *Apollo 6* photographs over a cold front. *Bull. Amer. Meteor. Soc.,* **56,** 4–16.

Spinhirne, J. D., and S. P. Palm, 1996: Space based atmospheric measurements by GLAS. *Advances in Atmospheric Remote Sensing with Lidar,* A. Ansmann et al., Eds., Springer-Verlag, 213–217.

——, M. Z. Hansen, and L. O. Caudill, 1982: Cloud top remote sensing by airborne LIDAR. *Appl. Opt.,* **21,** 1564–1571.

Szejwach, G., T. N. Sletten, and A. F. Hasler, 1983: The use of stereoscopic satellite observation in the determination of the emissivity of cirrus. *Adv. Space Res.,* **2,** 161–164.

Whitehead, V. S., I. D. Browne, and J. G. Garcia, 1969: Cloud height contouring from *Apollo 6* photography. *Bull. Amer. Meteor. Soc.,* **50,** 522–528.

Wylie, D. P., D. Santek, and D. O'C. Starr, 1998: Cloud-top heights from *GOES-8* and *GOES-9* stereoscopic imagery. *J. Appl. Meteor.,* **37,** 405–413.